Determination of phases of α-Fe_2O_3:SiO_2 compound by the rietveld refinement

S.A. Palomares Sánchez*
Istituto Materiali Speciali per Elettronica e Magnetismo (MASPEC)
Parco Area delle Scienze 37A-43010 Loc. Fontanni, Parma-Italia

S. Ponce-Castañeda and J.R. Martínez
Facultad de Ciencias, Universidad Autónoma de San Luis Potosí
78000 San Luis Potosí, S.L.P., México

Facundo Ruiz*
Instituto Potosino de Investigación Científica y Tecnológica
Av. V. Carranza 2025, San Luis Potosí, S.L.P., México

Recibido el 23 de abril de 2002; aceptado el 30 de julio de 2002

We use a variation of the Rietveld refinement method to calculate the amorphous content of composites formed by a silica xerogel amorphous matrix and iron particles embedded into. In order to apply the Rietveld refinement to amorphous structures an initial crystalline model is assumed with the same composition as the material to be modelled.
In this work we try to refine the structure of compounds using the program MAUD. It is shown how this program can be used to determine the amorphous and crystalline fractions in composites consisting of an amorphous matrix and incorporated iron oxide particles. The analysed compounds underwent different thermal treatments.

Keywords: Silicate glasses; sol-gel; structure; X-ray.

Se usa una variación del método de refinamiento Rietveld para calcular el porcentaje amorfo de compuestos formados por óxidos de fierro embebidos en una matriz amorfa de sílica xerogel. Para refinar la estructura amorfa, se parte de un modelo cristalino con la misma composición del material que se va a modelar. En este trabajo se pretende refinar la estructura de los compuestos usando el programa MAUD. Se muestra que el programa puede ser usado para determinar las fracciones amorfas y cristalinas en compuestos que consisten de una matriz amorfa con incorporación de partículas de óxido de fierro. El análisis de fases se realiza en muestras con diferentes tratamientos térmicos.

Descriptores: Vidrios silicatos; sol-gel; estructura; rayos-X.

PACS: 01.50.Pa; 81.20.Fw; 61.10.Yh

1. Introduction

The study of systems of particles embedded in inert matrixes has received a lot of attention due to their potential applications as materials with catalytic, optical and magnetic properties [1-7]. A lot of work has been done to research properties of magnetic systems based in iron nanocumuli, mainly of those systems with potential applications in magnetic recording, magnetic refrigeration, etc. In particular, maghemite has been widely used in magnetic recording systems and catalysis [8-12]; whereas hematite has been used in pigments, catalytic reactions and as anticorrosive agent [13].

An excellent supporting medium for magnetic iron oxide particles has been the SiO_2 matrix obtained using the sol-gel preparation method. Although it is observed that the magnetic properties of iron particles are modified, the interactions between the magnetic cumuli and the amorphous matrix are not yet well understood [14]. Possible magnetic mechanisms operating at the interfaces include dipole-dipole interactions, exchange, superexchange and magnetoelastic interactions and the occurrence of those interactions also depends on the microstructure. The study of structural changes induced by the incorporation of particles and by the thermal treatment could provide information on the interaction of these particles with the glassy matrix. A suggested way to perform such studies is first to determine the structure and then calculate some physical properties with the use of quantum mechanics formalism.

Several studies have been performed in order to investigate the structural and chemical properties of these systems, particularly by using infrared and Uv-Vis spectroscopy, and little effort has been done to refine the structural parameters of the glassy matrix and those of the incorporated particles [7,15-19].

The modelling of the silica glass has been introduced as a part of the general Rietveld refinement [20]. Among the programs that incorporate this routine is the so called ARITVE [20]. The assumption is that silica glass gives a diffraction pattern where it is not possible to distinguish if the structure is either completely amorphous or nanocrystalline. The method approximates the amorphous phase as a nanocrystalline solid where the long-range order is lost. The model is not sufficient to describe exactly the amorphous structure, moreover, from a fitting point of view, it provides nearly the same results as those obtained by reverse Monte Carlo simulation (RMC) [21]. In order to apply the Rietveld refinement to amorphous structures an initial crystalline model is assumed with the same composition as the material to be modelled. The Rietveld analysis of amorphous phases is based in an improved microcrystallinity model that includes micros-

trains. Using the Rietveld method for glass modelling supposes that one accepts the idea that a selected crystal structure may represent a mean model for a glass, or a nanocrystalline material. The disorder is statistically introduced by microstrain effect, leading to strong line broadening on the diffraction pattern.

The theoretical basis of the Rietveld analysis for amorphous samples is an improved microcrystallinity model of amorphous structures. According to the traditional microcrystallinity model, an amorphous solids consist of small domains with a crystalline structure. Le Bail included microstrains into the model, though in a phenomenological manner [21]. This method was first applied to multicomponent flouride glasses [23]. It was also applied to thin films of amorphous SiO_2 on Si-wafers in which data evaluation was made using the programs ARITVE [21] and LAXS [24]. For the thin films it was obtained the same spacegroup from synchrotron data, but different values of the lattice constant, namely **a** = 0.7055 nm.

It was also shown how this approach could be successfully used to determine the amorphous fraction in ceramic materials containing a glassy phase, and in synthetic mixtures of Al_2O_3 and SiO_2, where it is very important to assess the product quality by the check on the amorphous silica content [22].

For the first time, this method is used to refine the structure of composites of amorphous silica and embedded iron oxides, using the MAUD program. It applies the RITA/RISTA method [25,26]. The program was developed to analyse diffraction spectra and obtain crystal structures, quantity and microstructure of phases along with the texture and residual stresses. It is shown how this program can be used to determine the amorphous and crystalline fractions in composites consisting of an amorphous matrix with iron oxide particles incorporated into. The analyzed compounds underwent different thermal treatments.

2. Experimental procedure

The starting solutions for the formation of silica xerogel composites were prepared by mixing tetraethyl orthosilicate (TEOS), water, and ethanol. The mole ratios of ethanol to TEOS and water to TEOS were 4:1 and 11.67:1, respectively. Separately, a solution of $FeCl_3 \bullet 6H_2O$ were added to the solution at such amount that the metal oxide concentration, assuming full metal oxidation, is 30% wt. of the final dried powders. Soft pieces of the gels were obtained after 48 hr. Those pieces were ground to form a fine powder. For subsequent thermal treatment, the samples were placed in an oven at the desired temperature for 30 minutes, in air. Thermal treatments were performed at 400^{o}C, 600^{o}C, 800^{o}C, 1000^{o}C and 1100^{o}C.

X-ray diffraction patterns were obtained in a Rigaku 2200 diffractometer equipped with a nickel monochromator using Cu K_α(λ=1.54Å) radiation. Magnetization curves were obtained, at room temperature, using a LDJ 9600 vibrating sample magnetometer with H_{max} = 16 KOe. Further studies on these compounds are reported elsewhere [19].

X-ray data refinement was made using the program MAUD in order to calculate the amorphous/crystalline fraction of the composites [21]. The analysis was started assuming the structure of hematite (trigonal, spacegroup R-3c:H) for the iron oxide phase; and the structure of cubic SiO_2 (cubic, spacegroup $P2_13$) for the amorphous phase. For the crystalline phase of silica the structure of cristobalite (tetragonal, spacegroup $P4_12_12$) was assumed. All the used crystalline structures are already in the database of the MAUD program.

3. Results and discussion

Figure 1 shows the diffraction patterns of compounds of particles of iron oxide-silica at the indicated temperatures. Also the diffraction pattern of the sample without thermal treatment is shown. All the spectra show an overlap of the peaks around 23 $^\circ$ corresponding to the amorphous matrix of SiO_2. As the thermal treatment temperature increases to 400 $^\circ$C, new peaks appear whose position correspond to the hematite; this phase remains up to 1100 $^\circ$C. At this temperature, the crystalline phase of α-cristobalite appears indicating the change of phase of a small amount of amorphous silicon oxide. In order to calculate the amorphous/crystalline fraction of the composites, X-ray data refinement was made using the program MAUD.

Figure 2 shows the experimental pattern of the sample heat treated at 1000 $^\circ$C along with the fitted spectrum, using the MAUD program.

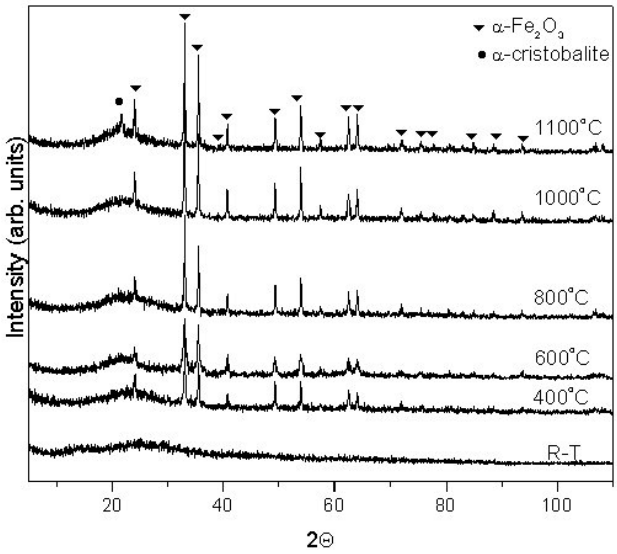

FIGURE 1. X-ray diffraction spectra of compounds of iron oxide particles embedded in a silica matrix at room temperature and heat-treated at the indicated temperatures.

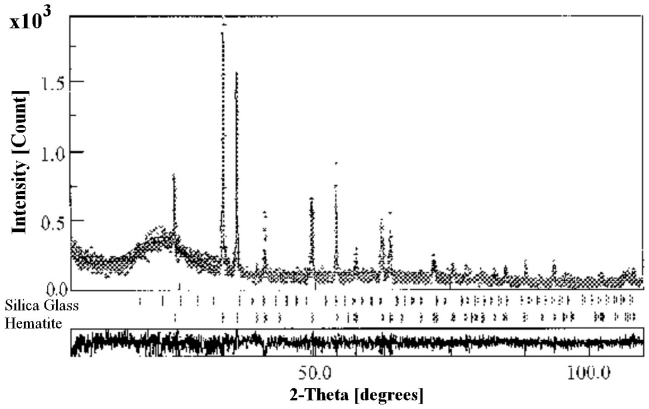

FIGURE 2. Experimental pattern of the sample heat treated at 1000 ˚ C along with the fitted spectrum.

The obtained quantitative analysis of the samples using the MAUD program are listed in Table I. The computed fraction of iron oxide is very near to the expected value. These results indicate that the used initial structural models give accurate results for the quantitative analysis of phases. The refinement were made only for quantitative analysis of phases, without structure refinement. An attempt to refine other iron oxide phases was made but the only detected phase corresponding to hematite. It is also possible that other iron compounds are present, but the resolution limit of this technique is unable to detect them when they are present in quantities less than 5% wt. [27].

TABLE I. Results of quantitative phase analyses of samples given in %.

	400 ˚ C	600 ˚ C	800 ˚ C	1000 ˚ C	1100 ˚ C
Hematite	15.16	31.00	28.14	32.83	29.62
$\alpha-$cristobalite	-	-	-	-	2.69
Amorphous silica	84.84	69.00	71.86	67.17	68.10

We reported at a previous work that the appearance of the hematite phase, when iron chloride is used as precursor, occurs at 400 ˚ C, and that small quantities of goethite as intermediate species are present [19]. Otherwise, the chloride decomposition occurs at temperatures above 400 ˚ C. The value in the phase content of hematite for the sample heat treated at 400 ˚ C, is reduced due to the presence of goethite and iron chloride.

Table II shows the atomic positions of atoms of the silica glass nanocrystalline structure for all the samples. These values are in good agreement with those of Ref. 21, where a more sophisticated study of the silica amorphous phase was made in samples of pure silica without addition of metalic agregates and without annealing. The structural cell parameters of hematite and cristobalite correspond to those expected because they are present as crystalline materials, (Table III).

Other refined parameters indicate that the refinement process gives good results about the amorphous/crystalline fraction of the composites. Also, the Si-O distance for cristobalite (1.601 Å) and the O-Si-O angle (109.5 ˚), and the mean Si-O distance for amorphous phase (1.620 Å and 1.615 Å for the samples annealed at 400 ˚ C and 1100 ˚ C, respectively) and the O-Si-O angle (109.7 ˚ and 109.5 ˚ the samples heat-treated at 400 ˚ C and 1100 ˚ C, respectively) are in good aggrement with the reported values [28] (respectively 1.608 $\pm$ 0.004 Å and 109.7 ˚ $\pm$ 0.6 ˚)

TABLE II. Atomic position of atom of silica glass. All the units are given in Å. Computation errors are $\pm$0,1%.

	A	$x_{Si(1)}$	$x_{Si(2)}$	$X_{O(1)}$	$x_{O(2)}$	$y_{O(2)}$	$z_{O(2)}$
Ref. 21	7.2025	0.27915	0.01574	0.1400	0.6367	0.6611	0.0603
400 ˚ C	7.2024	0.27914	0.01573	0.1399	0.6367	0.6611	0.0603
600 ˚ C	6.9034	0.28134	0.01590	0.1411	0.6398	0.6607	0.0596
800 ˚ C	7.0895	0.27937	0.01574	0.1399	0.6376	0.6614	0.0600
1000 ˚ C	7.0444	0.27422	0.01969	0.1525	0.6591	0.6497	0.0551
1100 ˚ C	7.1823	0.27932	0.01573	0.1399	0.6371	0.6607	0.0602

TABLE III. Cell parameters of hematite and cristobalite. Computation errors are $\pm$0,1%.

Hematite	1100 ˚ C	1000 ˚ C	800 ˚ C	600 ˚ C	400 ˚ C
a(Å)	5.03306	5.0341	5.0354	5.0346	5.0356
c(Å)	13.7451	13.7423	13.7743	13.7505	13.7489
Cristobalite					
a (Å)	5.0330	-	-	-	-

Variation in the fraction of iron oxide is expected, according to Infrared spectroscopy results that show the presence of free molecular water vibrations at temperatures up 600 ˚ C. The loss of water, combined with the growth of hematite phase that occurs in the range from 400 ˚ C to 1100 ˚ C, conduce to obtain different iron oxide content as a function of temperature. The variation of the content of iron oxide phase influences the magnetic properties of the samples.

Changes in the computed fraction of iron oxide are in relationship with the magnetic curves showed in Fig. 3, for the samples heat-treated at 400 ˚ C, 1000 ˚ C and 1100 ˚ C. In the figure is noticeable the change in shape of the hysteresis loops. In particular the saturation magnetization value decrease when the fraction of iron oxide diminish. The values of saturation magnetization in function of computed fraction of iron oxide are showed in Fig. 4. The reduction on the saturation magnetization is expected since this parameter depends on the total mass of the material embedded into silica matrix.

The magnetic parameters for the sample heat treated at 1100 ˚ C show a little change in their hope comportment. This situation is related to a structural change produced by the interaction of the hematite nanocluster with the silica gel matrix. At this temperatures start to appear crystallite cristobalite. For this case the saturation magnetization is reduced to about 0.06 emu/g, 25% lower that the saturation magnetization for the sample heat treated at 1000 ˚ C.

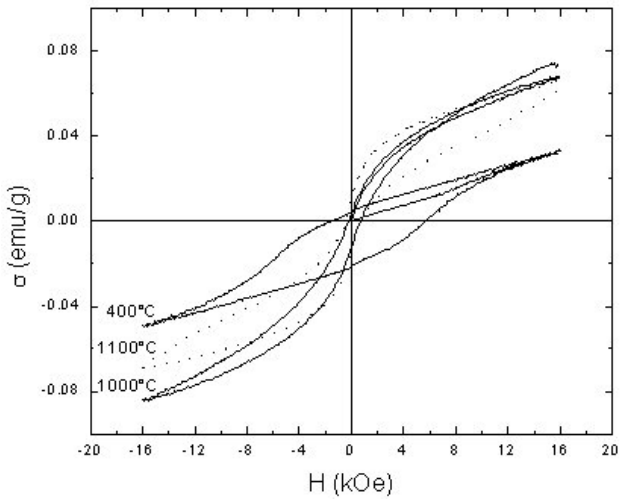

FIGURE 3. Magnetization curves for the sample heat-treated at 400 ˚ C, 1000 ˚ C and 1100 ˚ C.

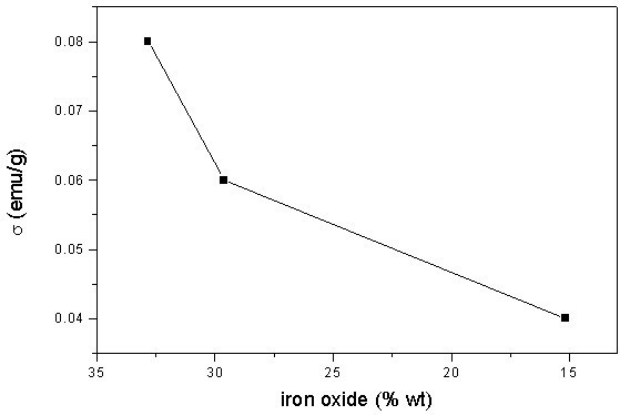

FIGURE 4. Saturation magnetization in function of computed fraction of iron oxide.

4. Conclusions

According to the results obtained in this work, it is possible the application of Rietveld refinement method to calculate the amorphous content of composites formed by an amorphous matrix and iron particles embedded into. It was also possible to calculate the amorphous/crystalline fraction in composites with two crystalline phases, as in the case of the sample heat-treated at 1100 ˚ C. In any case, very good agreement between experimental and calculated amorphous/crystalline fraction of composites was obtained. It does not mean, that the obtained refinement parameters describe the actual structure of the amorphous fraction of the samples, as happened with crystall-based models that fail to specify any local arrangement.

Although the Rietveld method is used to refine crystalline structures further improvement must be done in order to reproduce the amorphous structure of materials with models as simple as unitary cells.

Acknowledgements

The authors are indebted to Oscar Ayala-Valenzuela for magnetic measurements.

*. On sabbatical leave from UASLP.

1. H. Gleiter, *Prog. Mater. Sci.* **33** (1989) 223.
2. R.P. Andres, R.S. Averback, W.L. Brown, L.E. Brus, W.A. Godard III, A. Kaldor, S.G. Louie, M. Moscovits, P.S. Peercy, S.J. Riley, R.W. Siegel, F. Spaepen and Y. Wang, *J. Mater. Res.* **4** (1989) 704.
3. R.W. Siegel, in *Physics of new materials*, edited by F.E. Fujita (Springer, Heidelberg, 1994), pp. 65.
4. J.Y. Ying, A. Tschöpe, and D. Levin, *Nanostruct. Mater.* **6** (1995) 237.
5. F. Bentivegna, M. Nyvlt, J. Ferré, J.P. Jamet, A. Brun, ä. Viöovsky and R. Urban, *J. Appl. Phys.* **85** (1999) 2270.
6. M. Hayashi, M. Susa and K. Nagata, *J. Appl. Phys.* **85** (1999) 2257.
7. C. Cannas, D. Gatteschi, A. Musinu, G. Piccaluga and C. Sangregorio, *J. Phys. Chem. B* **102** (1998) 7721.
8. A.M Testa, S. Foglia, L. Suber, D. Fiorani, Ll. Casas, R. Roig, E. Molins, J. M. Grenèche and J. Tejada, *J. Appl. Phys.* **90** (2001) 1534.
9. S. Onodera, H. Kondo and T. Kawana, *MRS Bulletin* **21** (1996) 35.
10. M.H. Kryder, *MRS Bulletin* **21** (1996) 17.
11. H. Watanabe and J. Seto, *Bull. Chem. Soc. Jpn.* **61** (1991) 2411.
12. F. Hong, B.L. Yang, L.H. Schwartz and H.H. Kung, *J. Phys. Chem.* **88** (1984) 2525.
13. R.M. Cornell, and U. Schwertmann, *The iron oxides* (VCH Verlagsgesellschaft, Weinheim, Germany; VCH Publisher, New York, 1996), pp. 463.
14. J.P. Wang and H.L. Luo, *J. Appl. Phys.* **75** (1994) 7425.
15. S. Ramesh, I. Felner, Y. Koltypin, and A. Gedanken, *J. Mater. Res.* **15** (2000) 944.
16. K. Kandori, N. Ohkoshi, A. Yasukawa and T. Ishikawa, *J. Mater. Res.* **13** (1998) 1698.
17. Liping Li, Guangshe Li, R.L. Smith Jr. and H. Inomata, *Chem. Mater.* **12** (2000) 3705.
18. R.V. Morris, H.V. Lauer, C.A. Lawson, E.K. Gibson, G.A. Nace and C. Stewart, *J. Geophys. Res.* **90** (1985) 3126.
19. S. Ponce-Castañeda, J. R. Martínez, S. A. Palomares–Sánchez, F. Ruiz and O. Domínguez, *J. Sol-Gel Sci. & Techn.* (2000).

20. *The Rietveld method*, R. A. Young, Edit. International Union of Crystallography (Oxford University Press, New YorK, 1993).

21. A. Le Bail, *J. Non-Cryst. Solids* **183** (1995) 32.

22. L. Lutterotti, R. Ceccato, R. Dal Maschio and E. Pagani, *Mater. Sci. Forum* **278-281** (1998) 87.

23. A. Le Bail, C. Jacobini, R. de Pape, *J. Phys.* (Paris) *Coll.* **C8** (1985) 163.

24. P. Lecante, A. Mosset and J. Galy, *J. Of Appl. Crystall.* **18** (1985) 214.

25. H. R. Wenk, S. Matthies and L. Lutterotti, *Mater. Sci. Forum* **157-162** (1994) 473.

26. M. Ferrari and L. Lutterotti, *J. Appl. Phys.* **76** (1994) 7246.

27. B. D. Cullity. *Elements of X-ray diffraction* (Addison-Wesley. MA, 1978).

28. A.C. Wrigth, *J. Non-Cryst. Solids* **123** (1990) 129.